Controlling mechanisms of burning rate enhancement while using Flame Refluxer™ technology during in situ burning of crude oil spills

AUTHORS

Nathaniel Sauer

Principle Author, ngsauer@wpi.edu

Research Assistant, PhD Student, Worcester Polytechnic Institute

Combustion Lab, 100 Institute Road, Worcester Massachusetts 01609

Xiaoyue Pi, xpi@wpi.edu

PhD Student, Worcester Polytechnic Institute

50 Prescott Street, Worcester Massachusetts 01609

Kemal Arsava, ksarsava@wpi.edu

Research Engineer, Cold Regions Research and Engineering Laboratory

Hanover, New Hampshire 03755

Ali Rangwala, rangwala@wpi.edu

Professor of Fire Protection Engineering, Worcester Polytechnic Institute

50 Prescott Street, Worcester Massachusetts 01609

ABSTRACT #1141466

The focus of this study is to quantify the controlling mechanisms, which increases the burning rate of a pool fire using a Flame Refluxer™. Part of the Flame Refluxer™, is exposed to the fire and is heated up transferring heat to the fuel pool layer to which it extends. This enhances the conventional heat transfer that occurs only through the pool surface by transferring the heat from a fire to an in-depth layer of the liquid. Both sensible heat and heat of vaporization are supplied at increased rates by the submerged material. As an additional important effect, nucleate boiling onsets at the surface of the inserted material that generates bubbles of fuel vapor. These

bubbles are transported to the surface of the pool, where they burst and release the v0061por to the gas-phase. While doing so, additional processes such as formation of micron-sized droplets or small jets of liquid fuel from the break point occur. This phenomenon causes additional fuel in liquid phase transported to the gas-phase, where they vaporize, ignite and burn in heterogeneous mode. Therefore, the processes involved in FR occur in three steps; enhancement of heat transfer to the liquid causing nucleate boiling, formation of bubbles and their transport, and dynamics of bubble breakage at the pool surface causing transfer of liquid fuel in the form of tiny droplets or jets towards the gas-phase. This study analyzes the influence of bubbles on the burning behavior of a pool fire using a simple experiment involving burning ethanol as a fuel. Ethanol is used due to its transparency and hence bubble behavior is easily observable on the heater surface. A 5cm x 5cm glass enclosure constantly replenished with ethanol serves as the burning pool. A solid aluminum block (8.8 cm tall x 3.6 cm wide x 1.2 cm thick) is placed in the flame to act as the Flame Refluxer^{TM}. Bubble counts and burning rate measurements indicate the influence of the bubbles on the overall burning rate of the liquid pool.

INTRODUCTION

Burning of crude oil is an area of expanding interest in the modern world. In-situ burning is a cleanup process by which spilled crude oil or other flammable liquids are burned in place on the waters' surface (Mullin & Champ, 2003). This process is quick, effective, and low-cost. The Flame Refluxer^{TM} (FR) is a technology developed to enhance this in-situ burning process by "recycling" as much of the heat energy produced by the fire as possible (Patent No. US20180149356A1, 2018; Patent No. US20190127937A1, 2019; Patent No. US9772108B2, 2015; Arsava et al., 2018; Arsava et al., n.d.). Flame Refluxer^{TM} technology would be deployed in an in-situ burning environment in order to increase the speed, efficiency, and cleanup ability of in-

situ burning. As shown in Fig. 1, the FR is composed of two main components the ‘collector’ and the ‘heater’. The collector is in the flame region and collects heat energy from the flame by means of convection and radiation from the hot combusting plume. The heater and collector are physically connected and made from high thermal conductivity materials, usually copper. Thus, heat is transferred down the collector and into the heater which is in the liquid fuel region. Heat energy is then convectively transferred back into the liquid fuel region. This added energy increases the mass transfer of the liquid fuel, allowing more ready vaporization and thus increasing the burning rate of the fuel. In addition, if the temperature of the heater is more than the boiling point of the liquid nucleate boiling will also occur on the surface. The current study shows how the nucleate boiling further contributes to the increase in the burning rate of the fuel. It should be noted that the physical effects analyzed in this study are beyond the enhancement in the convective heat transfer usually associated with nucleate boiling in two phase flow and described for example in Sezer et al. (Sezer, Arsava, Kozhumal, & Rangwala, 2017).

During nucleate boiling liquid fuel changes phase into vapor at nucleation sites on the heater surface (Fig. 1). As these bubbles reach the surface of the liquid and pop, they contribute to an increase in burning rate by three modes:

1. First, these bubbles contain fuel vapor, which is immediately released once the bubbles bursts on the surface of the fuel.
2. Second, the bubbles pop and produce jet-drops or a multitude of smaller fuel drops called ‘film drops’ as shown in Fig. 1. These smaller drops are ejected from the fuel surface and towards the gas-phase where they vaporize and combust, further contributing towards the burning rate.

3. Third, a pressure wave is created when the bubbles burst on the fuel surface. Which facilitates mass transfer of the liquid in the immediate vicinity of the bubble because of increased convection.

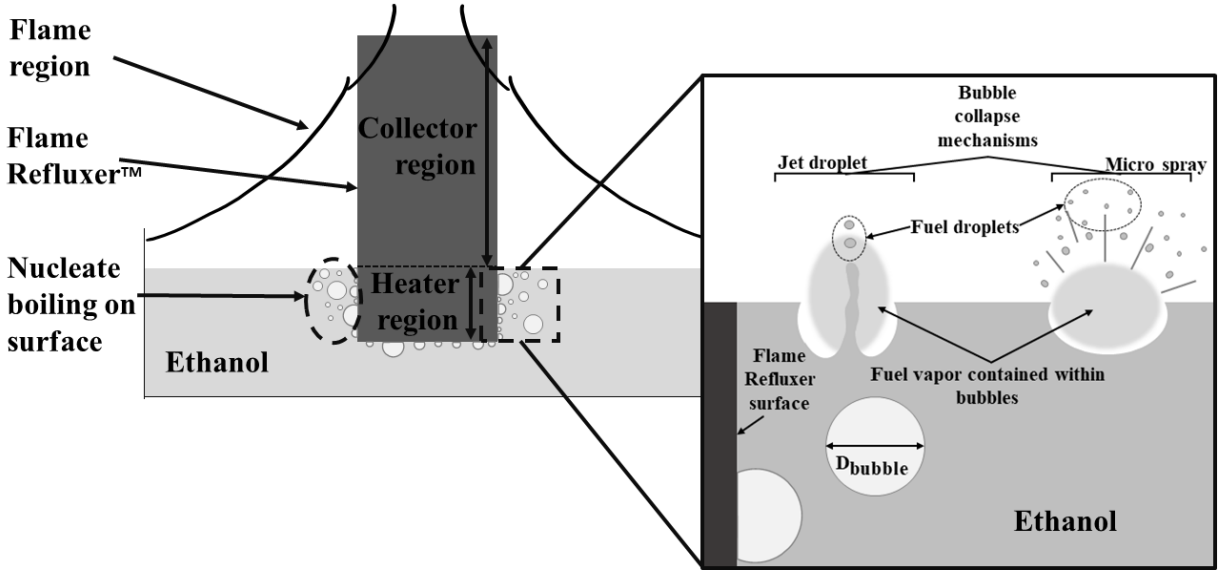

Figure 1 – Schematic of the Flame Refluxer™ (FR) showing the two main components: heater and collector. The inset shows bubble collapse dynamics contributing to additional fuel vapor release.

Understanding how the addition of bubbles contributes to the burning behavior of a pool fire is important. Prior studies have examined how the influence of bubbles, or various methods to control bubbles, can increase heat transfer from a heater to a liquid (Chi-Yeh & Griffith, 1965; Sezer et al., 2017; Ujereh, Fisher, & Mudawar, 2007; Webb, 1981). As well studies have also investigated how and what type of bubbles produce different sizes of droplets that are ejected from the liquid surface as shown in Fig. 1 (Li, Miller, Wang, Koley, & Katz, 2017; Murphy, Li, d'Albignac, Morra, & Katz, 2015; Poulain, Villermaux, & Bourouiba, 2018; Spiel, 1995). However, no studies have investigated the influence of bubbles on the burning rate of a liquid pool fire. This forms the primary motivation for the current study.

METHODOLOGY

The experimental setup consists of a 5cm x 5cm glass enclosure being constantly replenished with ethanol by a continuous filling source (Fig. 2). These two vessels are connected via a tube, and atmospheric pressure ensures that the fuel level in the burning vessel remains the same as in the filling vessel. The filling vessel is being constantly filled and drained such that it always remains at the same height. Ethanol is pumped into the constantly replenished loop by an OMEGA FPU5MT peristaltic pump set to a constant flow rate. The overflow container is placed on a Sartorius ED6202S-CW load cell to measure the amount of fuel consumed (Capacity of 6.2 kg with a sensitivity of 0.01 g and a factory uncertainty of ±0.03 g). High framerate video was recorded with a Panasonic Lumix FZ300 filming at 240 fps.

A solid block of aluminum (8.8 cm tall x 3.6 cm wide x 1.2 cm thick) weighing 112 grams is used as the FR for these experiments and is submerged 2cm into the ethanol pool (Fig 2.). The aluminum block is held in place by a ceramic rod inserted into a small hole in the block and attached to a stand. This method ensures low heat loss from the aluminum block to the ceramic rod and stand. This small and uniform aluminum block was chosen for bubble visualization and ease of calculating surface area as compared to for example porous materials. There is a correlation between improvement to burning rate and the ratio of heater area to pool area which will be further examined in the results and discussion section.

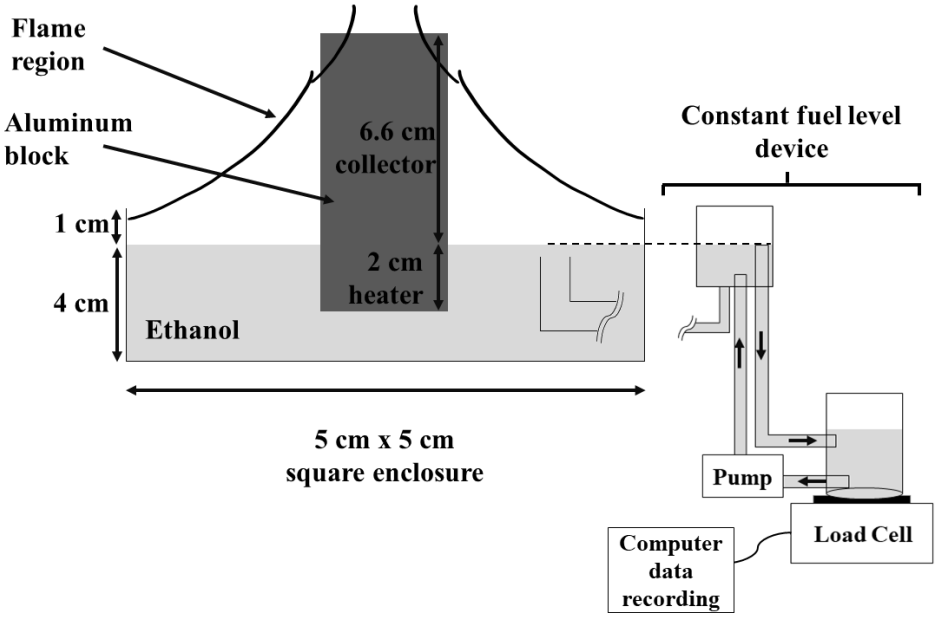

Figure 2 - Experimental set up.

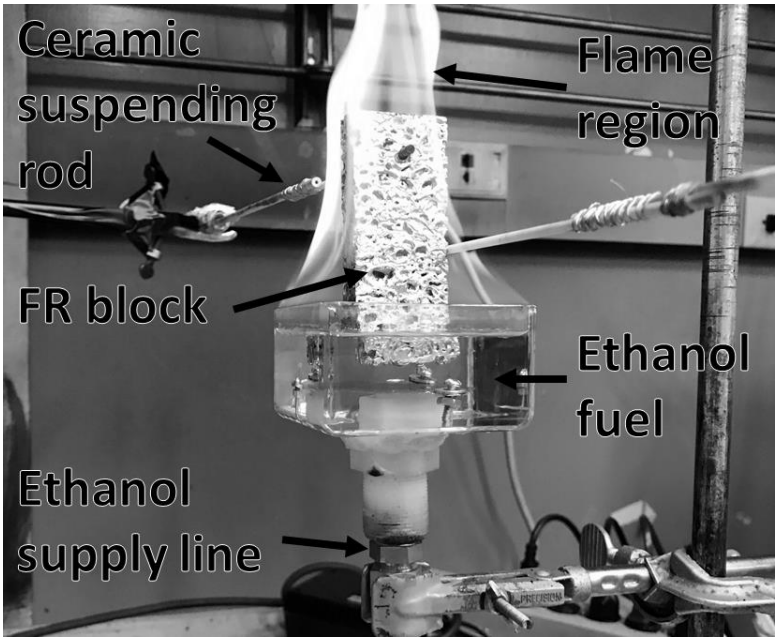

Figure 3 - Picture showing an experimental Flame Refluxer™ (data not referenced in this study) immersed in the burning pool of constantly replenished ethanol fuel.

The ethanol pool was burned in three separate trials with no aluminum block to establish a baseline burning rate. Then again in three independent trials with the aluminum block to establish

an average enhanced burning rate. Data consists of mass loss data collected from the load cell, providing an accurate experimental measurement of mass loss rate (burning rate) over time. Videos are also collected for analysis from each experiment. Videos from the trials with the FR are used to count and analyze bubbles induced by the FR. At a time sufficiently into the experiment to ensure steady state; a size and frequency count of bubbles produced by the FR is analyzed using the videos taken of the experimental trial. This bubble analysis is then used to determine the potential contribution of bubble popping to the burning rate enhancement.

RESULTS AND DISCUSSION

Addition of a FR to a pool fire significantly enhances the burning rate as shown in Fig. 4. For the 5cm x 5cm ethanol pool fire, burning rate was enhanced to over 3 times the baseline burning rate, from 0.04 g/s to 0.13 g/s with the FR.

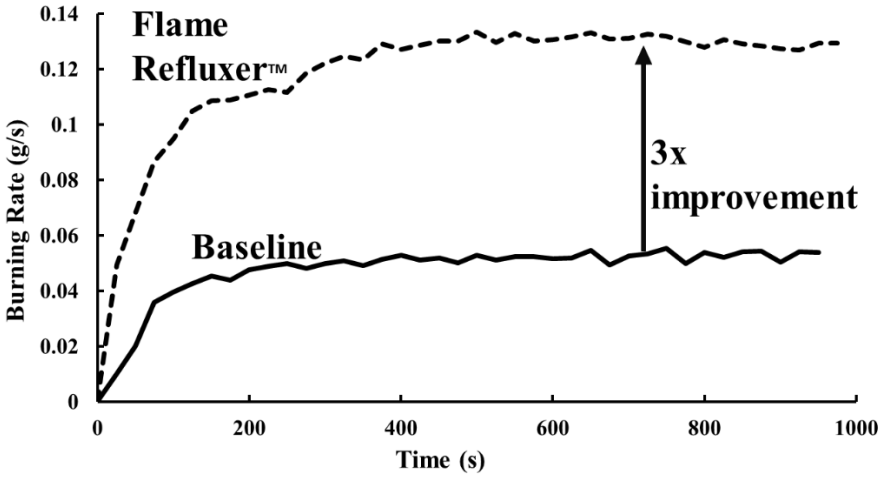

Figure 4 - Baseline and FR burning rate as a function of time. The FR increases the burning rate by a factor of 3.

For small convective limit pool fires it is known from Babrauskus (Babrauskas, 1983) that mass loss rate (burning rate) can be represented by the heat input into the fuel divided by the heat of gasification of the pool. Using this correlation (equation 1) and the average experimental

burning rate for the baseline, the heat is transferred back to the fuel to sustain natural burning (baseline conditions) can be estimated (*Latent Heat,* $\Delta h_{g,ethanol} = 0.918$ kJ/g) (Perry, R.H., Green, 2004).

$$\dot{m}'' = \frac{\dot{q}''}{\Delta h_g}, \quad (1)$$

$$\dot{q}'' = \dot{m}'' \times \Delta h_g = 0.04 \text{ g/s} \times 0.918 \text{ kJ/g} = 37 \frac{J}{s}.$$

For the baseline burning rate 37 Joules of energy is transferred back to the fuel naturally by radiation and convection. This energy is utilized in vaporizing fuel to sustain combustion. Thus, naturally increasing the burning rate can be accomplished by increasing the amount of energy returned to the fuel. However, the FR has further mechanisms of improvement due to the nucleate boiling which occurs on the FR surface. The improvement that the FR offers over the baseline is known. In order to break this improvement down into its pieces, the bubbles must first be examined.

Impact of the bubbles:

In this study the impact of the bubbles on the burning rate is mathematically analyzed by first obtaining bubble measurements from high-speed video, then using these measurements to evaluate accurate approximations for each mechanism.

Analysis of high-speed image data from the burning experiments revealed three different classes of bubbles produced on the heater surface. Fig. 5 shows a sample photograph during the experiment. The three types of bubbles classified based on an average size and frequency (*f)* are shown in the photograph. The largest bubbles produced are about 9 mm in diameter and are produced at a frequency of 21.3 bubbles per second. Medium sized bubbles around 4 mm are produced at a frequency of 130 bubbles per second. Finally, the smallest bubbles which are

produced the most frequently are less than 1 mm in size. These vary the most in size and production but are generally on the order of 0.5 mm in size and produced at a frequency of about 1,000 bubbles per second. Using this bubble frequency and size information, estimations for the contribution to burning rate of each mechanism are now possible.

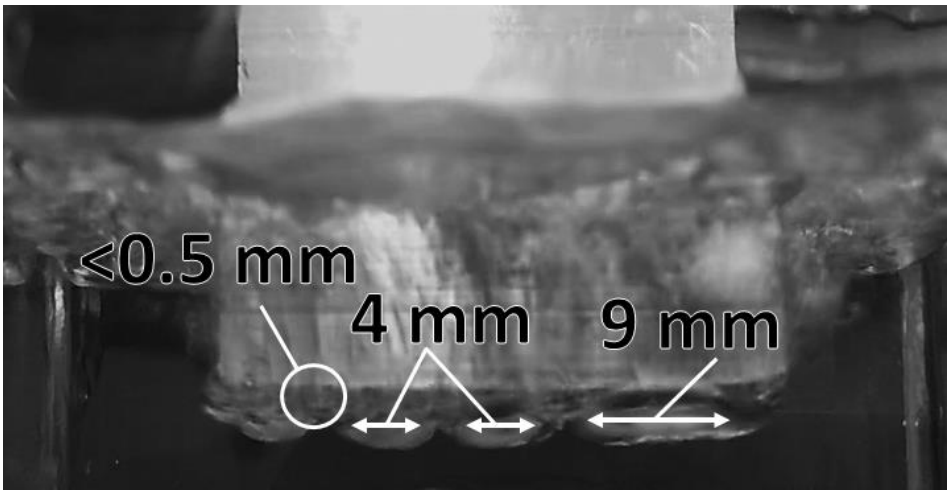

Figure 5 - Picture of nucleate boiling occurring on the heater surface during an experiment, various bubble sizes marked.

First, an estimation of the amount of fuel vapor produced by the popping bubbles is conducted. Assumptions include each of the three bubble classes is spherical in size, and the density of fuel vapor in every bubble is consistent at (0.00159 g/cm^3) (Perry, R.H., Green, 2004). Using these assumptions, multiplying the spherical volume of each bubble class, by its average generation frequency (*f*), and then by the density of ethanol vapor provides vapor production due to the bubbles as shown in equation 2.

$$\frac{4}{3}\pi r^3 \times f \times \rho_{eth.vapor} = \dot{m}_{vap}\frac{g}{s}. \quad 2$$

In order to estimate the contribution of the film droplets produced by the popping bubbles, estimates for the size of film droplets produced when the bubbles pop is needed. Due to the highly turbulent fuel surface and the obstruction of view of the surface from the metal block, imagery of

the film droplets produced by bubbles popping could not be obtained in these experiments. Spiel (Spiel, 1995) provides detailed film droplet size distributions for various bubble sizes which will be used to estimate the size of droplets produced by the popping bubbles. However, it should be noted that Spiel's experiments were conducted in seawater, and the differences in the properties of seawater and ethanol will play a role in the size of film droplets produced, if only on the order of fractions of a millimeter.

Spiel (Spiel, 1995) gives droplet distributions for both the number and size of film drops produced per bubble size that produces them. Spiel found that bubbles about 9mm in diameter will produce 70 film drops per burst each 100 microns in diameter. As well bubbles 4 mm in diameter will produce 20 film drops per burst each 20 micrometers in diameter. Spiel found that ultra-fine bubbles less than 1 mm in diameter did not produce film drops, or at least any of measurable size, which is consistent with observations from these experiments. To calculate the mass loss contribution from the film drops produced, multiply the bubble frequency (*f*) by the film drop production frequency then average film drop size and finally by ethanol liquid density (0.79 g/cm^3) (Perry, R.H., Green, 2004) as shown in equation 3.

$$f \times \frac{\text{film drops}}{\text{bubble}} \times \frac{4}{3}\pi r^3 \times \rho_{\text{eth.liquid}} = \dot{m}_{\text{burst}} \frac{\text{g}}{\text{s}}. \qquad 3$$

Equation 2 and 3 are used to calculate the additional contribution to the fuel vapor because of bubbles popping and releasing vapor at the surface ($\dot{m}_{vap}$) and because of micron sized droplets forming because of bubble burst ($\dot{m}_{burst}$). The contribution to the mass loss rate by the three different bubble sizes observed experimentally is shown in Table 1.

Table 1 - Contribution in (g/s) of the vapor and droplet production for each bubble size. Far right column shows percent contribution of the vapor and droplets for each bubble size towards the overall improvement of 0.09 g/s over the baseline.

Bubble Size (mm)	Bubble Frequency *f*	$\dot{m}_{vap}$ g/s	$\dot{m}_{burst}$ g/s	**Combined Contribution (% of 0.09 g/s)**
Large (9)	21.33	0.013	0.005	20%
Medium (4)	130	0.007	0.0002	8%
Small (less than 0.50)	1000	0.0001	-	0.1%
Total	-	0.021	0.0052	28.1%

Remembering that the original burning rate without a FR or bubbles was 0.04 g/s and with a FR the burning rate improved to 0.13 g/s, the overall improvement over the baseline is 0.09 g/s which is used for comparison in the last column in Table 1. Further, table 1 shows that even though the number and frequency of large bubbles (9 mm) is the smallest, their contribution towards the promotion of mass burning rate is the highest. For example, at 21 bubbles per second, the 9 mm diameter bubbles provide 0.013 g/s of fuel vapor, which is ~32% of the fuel vapor generated during the baseline burn (0.04 g/s). If the number of large bubbles were doubled, by say adding one more aluminum block in the pool, the corresponding quantity of fuel vapor would have also doubled to 64%. The medium sized (~ 4 mm) bubble contribution is approximately half that of the larger bubbles, even though their frequency is five times higher. As shown in Table 1, the smallest size bubbles (< 0.5 mm) seem to have a negligible influence on the fuel vapor addition. However, it is possible that they may have an important role in enhancing the mass transfer by bursting dynamics (Lasheras, Fernandez-Pello, & Dryer, 1980).

Extrapolating an error magnitude for these approximations is difficult. No experimental data has been collected on the actual mass transferred by these mechanisms, and further complex experiments would be required to isolate each mechanism and measure its mass contribution

individually. However, an estimate for magnitude of error can be made for example due to an erroneous bubble count. An error in the large bubble counting resulting in a 2 bubbles/ second difference between observed and actual bubble frequency would lead to a ±7% difference in observed vapor mass flux. This process was repeated for medium and small bubbles as shown in table 2. As can be seen the variance for each of the bubbles due to an erroneous bubble count is relatively small. This is because bubble count is only multiplied into the bubble size. Bubble size will play a much larger role in induced error as this value is cubed. Therefore, measurement of the bubble sizes must be completed as accurately as possible.

Table 2 - Change in bubble frequency and the resulting change in $\dot{m}_{vap}$ and $\dot{m}_{burst}$.

Bubble Size	**Difference in f from measured (bubbles/sec)**	Change in $\dot{m}_{vap}$ g/s	Change in $\dot{m}_{burst}$ g/s
Large (9)	2	±1E-3	±5E-4
Medium (4)	10	±5E-4	±5E-6
Small (less than 0.50)	1000	±8E-4	-

With 28.1% of the improvement to burning rate accounted for, the rest of the improvement can now be explained. The third mechanism, increased convective movement by bubble pressure waves, is not an observable phenomenon or measurable by means available in this experiment. Therefore, this improvement mechanism is 'lumped' with the final improvement mechanism, the added sensible and latent heat energy. That is some of the remaining 72% improvement is due to this enhanced convective movement, but for the purpose of estimating the final calculable mechanism, it will be ignored. Thus, this final improvement will be assumed to be due to heat energy added to the fuel layer by the FR. Using equation 1 as before, estimating then amount of heat energy returned by the FR is now possible. However, first the energy used to create the bubble vapor must be accounted for.

$$\text{Energy used to create bubbles} = \text{Total Bubble Vapor}\left(\frac{g}{s}\right) \times \Delta h_g \left(\frac{kJ}{g}\right),$$

$$0.021 \times 0.918 \left(\frac{kJ}{g}\right) = 18.45 \ \frac{J}{s}\ .$$

Again, using equation 1 as before to estimate the heat returned to the fuel by the FR in order to constitute the rest of the improvement to burning rate.

$$\dot{m}'' = \frac{\dot{q}''}{\Delta h_g},$$

$$0.0647 \ \frac{g}{s} = \frac{\dot{q}''}{0.918 \frac{kJ}{g}}; \ \dot{q}'' = 59.4 \ \frac{J}{s},$$

$$E_{total} = 59.4 + 18.45 = 77.85 \ \frac{J}{s}.$$

The energy rate brought back to the fuel layer by the FR is 77.85 Joules per second. This is 2 times the rate returned to the fuel by natural means in the baseline case (37 J/s). This demonstrates that a single aluminum block can return double the amount of energy to the fuel compared to a naturally burning pool fire. This addition improves burning rate by a factor of 3 (Fig. 4). Of the improvement mechanisms 72% of the burning rate improvement is because of an improvement in mass transfer because of additional heating to the fuel by conduction from the FR. The remaining 28% improvement is because of bubble dynamics caused by nucleate boiling. First, these bubbles contain fuel vapor, which is immediately released once these bubbles bursts on the surface of the fuel. Second, the bubbles pop and produce jet-drops or a multitude of smaller fuel drops called ‘film drops’ as shown in Fig. 1. These smaller drops are ejected from the fuel surface and towards the gas-phase where they vaporize and combust, further contributing towards the burning rate. Third, a pressure wave is created when the bubbles bursts on the fuel surface. Which

facilitates mass transfer of the liquid in the immediate vicinity of the bubble because of increased convection.

These results are significant because they demonstrate not only the effectiveness of the FR, but also the previously unaccounted for impact of a boiling fuel on pool fire burning rate. The bubbles have a significant and consequential impact on the burning rate in these experiments. These experiments were also at a small scale, with a relatively small bubbles at low generation frequencies. Adding further FR could dramatically increase the burning rate enhancement, as well as preparing the surface to encourage nucleate boiling. Further studies are needed to examine the impact of the bubbles in detail. For example, investigating the ability of various bubble sizes to produce droplets in different homogenous and multicomponent fuels.

Ethanol is used in these experiments due to its ease of use, clarity, and well-established properties. However, crude oil is the operating fuel condition for the Flame Refluxer^{TM} technology. Crude oil is a multicomponent mixture, containing a variety of liquid fuels and even some solids. Some of these fuels will be more volatile than ethanol while other will be less volatile. The effect of a multicomponent fuel on bubble generation on the heater surface, and on the burning rate enhancement mechanisms detailed in this study is unknown.

The effect of the varied physical properties of different fuels on these mechanisms is unknown. For example, a higher viscosity fuel could produce more droplets due to formation of a thicker bubble cap and thus more liquid fuel available to form into film droplets upon bubble bursting. However, a higher viscosity could also mean that bubbles would have a delayed burst upon reaching the surface. A delayed burst could cause an accumulation of bubbles, but also a film of bubbles would increase fuel surface area as well as heat more quickly than the bulk fuel layer. These competing factors make a quantitative estimate challenging. Suffice to say that the 28%

obtained using the single component fuel like ethanol used in the current study can increase or decrease depending on the nature of the crude oil being burned.

Additionally, we hypothesize heat transfer during these experiments is taking place in the lower end of the regime of sub-cooled nucleate boiling. Sub-cooled nucleate boiling represents an enhanced but not maximized heat transfer rate from the solid to the liquid. From the energy return rate to the fuel as calculate above, we can estimate the Heat Flux (kW/m^2) across the surface area of the FR to be around 30 kW/m^2. The nucleate boiling curve from Hao et al. for ethanol boiling on a smooth heated surface places this heat flux value in the sub-cooled nucleate boiling region as expected. This nucleate boiling curve also reveals the heat transfer coefficient for our experiments is low (3-4 kW/m^2K), and could improve to 3 times this value at the peak critical heat flux (Hao, Wang, Jiang, Guo, & Guo, 2017). This proves that much more improvement, possibly upwards of 10 times the baseline burn rate, lies within the FR's reach. Increasing the surface area by adding more solid blocks to the pool, would lead to even further improvements to the burning rate. Additional FR blocks and maximizing the heat transfer coefficient was not examined in this study as the focus was on the bubbles contribution to burning rate. With additional FR blocks observation would become more difficult with a cluttered pool and more turbulent fuel surface.

Despite the unknowns, a major contribution of this study is that the enhancement mechanisms detailed in this study induced by popping bubbles has now been established. How this enhancement will vary with increasing submerged heater area, fuel viscosity and multicomponent fuels requires further investigation.

CONCLUSIONS

Experiments are conducted to evaluate the contributing mechanisms of a submerged Flame Refluxer™ on the burning rate of a pool fire. Three previously unaccounted for mechanisms are found to contribute to mass loss enhancement:

1. Bubbles containing fuel vapor, which is immediately released once the bubbles bursts on the surface of the fuel.
2. Bubbles popping and producing jet-drops, or a multitude of smaller fuel drops called 'film drops' as shown in Fig. 1. These smaller drops are ejected from the fuel surface and towards the gas-phase where they vaporize and combust, further contributing towards the burning rate.
3. A pressure wave is created when the bubbles burst on the fuel surface. Which facilitates mass transfer of the liquid in the immediate vicinity of the bubble because of increased convection.

Using high-speed video analysis estimations for the contributions to mass loss rate are made for the first two mechanisms. Vapor contained within the bubbles and droplets produced by the bursting bubbles was found to contribute up to 28% of the overall enhancement to burning rate. Enhanced convection due to pressure waves created by popping bubbles could not be measured and will require further investigation. The FR was found to increase the amount of energy returned to the fuel by more than 2 times. The increase in burning rate can be mostly attributed to the added latent heat returned by the FR, to the fuel pool. However, this study demonstrates that previously unaccounted for mechanisms induced by bursting bubbles, contribute in a substantial manner to burning rate enhancement. Further studies to systematically isolate each mechanism to experimentally measure their contribution are needed.

ACKNOWLEDGEMENTS

This work was supported by the Department of the Interior Grant E140E0118R0007. The contents do not necessarily reflect the views and policies of the BSEE, nor does mention of the trade names or commercial products constitute endorsement or recommendation for use.

REFERENCES

Arava, S., Arsava, K., Rangwala, A., Sezer, H., Walawalkar, A., & Raghavan, V. (2018). *Patent No. US20180149356A1*. United States.

Arsava, K., Raghavan, V., & Rangwala, A. (2018). Enhanced Oil Spill Clean-Up Using Immersed Thermally Conductive Objects. *Fire Technology, 54*. https://doi.org/10.1007/s10694-018-0767-2

Arsava, K., Rangwala, A., & Mahnken, G. (2019). *Patent No. US20190127937A1*. Retrieved from https://patents.google.com/patent/US20190127937A1/en

Arsava, K., Tukaew, P., Borth, T., Petrow, D., Kozhumal, S. P., Mahnken, G., … Torero, J. L. (n.d.). *Enhanced Burning of Oil Slicks*.

Babrauskas, V. (1983). *Estimating large pool fire burning rates* (Vol. 19). https://doi.org/10.1007/BF02380810

Chi-Yeh, H., & Griffith, P. (1965). The mechanism of heat transfer in nucleate pool boiling. *International Journal of Heat and Mass Transfer, 8*(6), 887–904. https://doi.org/https://doi.org/10.1016/0017-9310(65)90073-6

Hao, W., Wang, T., Jiang, Y. yan, Guo, C., & Guo, C. hong. (2017). Pool boiling heat transfer on deformable structures made of shape-memory-alloys. *International Journal of Heat and Mass Transfer, 112*, 236–247. https://doi.org/10.1016/j.ijheatmasstransfer.2017.04.113

Lasheras, J. C., Fernandez-Pello, A. C., & Dryer, F. L. (1980). Experimental Observations on the Disruptive Combustion of Free Droplets of Multicomponent Fuels. *Combustion Science and*

Technology, *22*(5–6), 195–209. https://doi.org/10.1080/00102208008952383

Li, C., Miller, J., Wang, J., Koley, S. S., & Katz, J. (2017). Size Distribution and Dispersion of Droplets Generated by Impingement of Breaking Waves on Oil Slicks. *Journal of Geophysical Research: Oceans*, *122*(10), 7938–7957. https://doi.org/10.1002/2017JC013193

Mullin, J. V, & Champ, M. A. (2003). Introduction/Overview to In Situ Burning of Oil Spills. *Spill Science & Technology Bulletin*, *8*(4), 323–330. https://doi.org/https://doi.org/10.1016/S1353-2561(03)00076-8

Murphy, D. W., Li, C., d'Albignac, V., Morra, D., & Katz, J. (2015). Splash behaviour and oily marine aerosol production by raindrops impacting oil slicks. *Journal of Fluid Mechanics*, *780*, 536–577. https://doi.org/10.1017/jfm.2015.431

Perry, R.H., Green, D. W. (2004). Perry's Chemical Engineers' Handbook (8th rev. ed.). In *Perrys' chemical engineers' handbook*. https://doi.org/10.1036/0071511245

Poulain, S., Villermaux, E., & Bourouiba, L. (2018). Ageing and burst of surface bubbles. *Journal of Fluid Mechanics*, *851*, 636–671. https://doi.org/10.1017/jfm.2018.471

Rangwala, A. S., Shi, X., Arsava, K. S., & Mahnken, G. (2015). *Patent No. US9772108B2*. Retrieved from https://patents.google.com/patent/US9772108B2/en

Sezer, H., Arsava, K. S., Kozhumal, S. P., & Rangwala, A. S. (2017). The effect of embedded objects on pool fire burning behavior. *International Journal of Heat and Mass Transfer*, *108*, 537–548. https://doi.org/https://doi.org/10.1016/j.ijheatmasstransfer.2016.12.021

Spiel, D. E. (1995). On the births of jet drops from bubbles bursting on water surfaces. *Journal of Geophysical Research: Oceans*, *100*(C3), 4995–5006. https://doi.org/10.1029/94JC03055

Ujereh, S., Fisher, T., & Mudawar, I. (2007). Effects of carbon nanotube arrays on nucleate pool

boiling. *International Journal of Heat and Mass Transfer*, *50*(19), 4023–4038. https://doi.org/https://doi.org/10.1016/j.ijheatmasstransfer.2007.01.030

Webb, R. L. (1981). The Evolution of Enhanced Surface Geometries for Nucleate Boiling. *Heat Transfer Engineering*, *2*(3–4), 46–69. https://doi.org/10.1080/01457638108962760